blood®
Regular Article

THROMBOSIS AND HEMOSTASIS

PAR4 activation involves extracellular loop 3 and transmembrane residue Thr153

Xu Han,[1] Lukas Hofmann,[1] Maria de la Fuente,[1] Nathan Alexander,[1] Krzysztof Palczewski,[2] the INVENT Consortium, and Marvin T. Nieman[1]

[1]Case Western Reserve University, School of Medicine, Cleveland, OH; and [2]University of California, Irvine, School of Medicine, Irvine, CA

KEY POINTS

- PAR4 activation requires a coordinated rearrangement of ECL3 and Thr153 in the tethered LBS formed by TM3 and TM7.
- PAR4 Leu310 (rs2227376) in ECL3 has lower receptor reactivity compared with Pro310 and correlates with reduced VTE risk in GWAS analysis.

Protease-activated receptor 4 (PAR4) mediates sustained thrombin signaling in platelets and is required for a stable thrombus. PAR4 is activated by proteolysis of the N terminus to expose a tethered ligand. The structural basis for PAR4 activation and the location of its ligand binding site (LBS) are unknown. Using hydrogen/deuterium exchange (H/D exchange), computational modeling, and signaling studies, we determined the molecular mechanism for tethered ligand–mediated PAR4 activation. H/D exchange identified that the LBS is composed of transmembrane 3 (TM3) domain and TM7. Unbiased computational modeling further predicted an interaction between Gly48 from the tethered ligand and Thr153 from the LBS. Mutating Thr153 significantly decreased PAR4 signaling. H/D exchange and modeling also showed that extracellular loop 3 (ECL3) serves as a gatekeeper for the interaction between the tethered ligand and LBS. A naturally occurring sequence variant (P310L, rs2227376) and 2 experimental mutations (S311A and P312L) determined that the rigidity conferred by prolines in ECL3 are essential for PAR4 activation. Finally, we examined the role of the polymorphism at position 310 in venous thromboembolism (VTE) using the International Network Against Venous Thrombosis (INVENT) consortium multi-ancestry genome-wide association study (GWAS) meta-analysis. Individuals with the PAR4 Leu310 allele had a 15% reduction in relative risk for VTE (odds ratio, 0.85; 95% confidence interval, 0.77-0.94) compared with the Pro310 allele. These data are consistent with our H/D exchange, molecular modeling, and signaling studies. In conclusion, we have uncovered the structural basis for PAR4 activation and identified a previously unrecognized role for PAR4 in VTE. (*Blood*. 2020;136(19):2217-2228)

Introduction

Protease initiated signaling events are essential for many physiological processes such as platelet aggregation, inflammatory signaling, and regulation of endothelial barrier function.[1-3] Protease-activated receptors (PARs) are primary mediators that transmit signal transduction from the protease to the intracellular signaling machinery. The 4 PAR members, PAR1, -2, -3, and -4, are expressed in many cell types and are activated by a growing panel of proteases.[4-8] PARs are activated by enzymatic cleavage of the N terminus to expose a tethered ligand.[4,9,10] Compared with a soluble ligand, the attached tethered ligand reduces the increase in entropy upon dissociation, resulting in an entropy-driven higher affinity for PAR activation. This activation mechanism creates unique challenges in targeting PARs therapeutically. Furthermore, because the ligand is attached to the receptor, there are likely substantial conformational changes that occur during PAR activation. These structural rearrangements and the precise mechanism of this unique protein-tethered ligand interaction are unknown.

PAR4 has primarily been studied on platelets where it is co-expressed with PAR1. Together they mediate the full spectrum of thrombin signaling.[11] PAR1 is efficiently cleaved by thrombin and mediates rapid transient signaling. In contrast, PAR4 leads to prolonged signaling and sustained platelet activation. Recently, these differences in signaling kinetics have been exploited therapeutically. Blocking PAR4 spares the rapid response mediated by PAR1 thereby limiting the bleeding complications.[12] In addition, polymorphisms in the PAR4 gene (*f2rl3*) lead to sequence variants that impact its signaling and response to some antagonists.[13] PAR4 therapies have focused on coronary artery disease. However, there is growing evidence that platelets have a key initiating role in venous thromboembolism (VTE). Despite the key role of PAR4 in platelet biology, its role in VTE and potential as a therapeutic target are unknown.

Despite numerous studies of PAR function, the understanding of the structural basis for the tethered ligand has been limited to nuclear magnetic resonance imaging of the isolated N-terminal exodomain of PAR1 in solution and the crystal structure of PAR1 or PAR2 bound to antagonist.[14-16] The major limitation of the crystallization studies is the need for significant modifications to stabilize the receptor in a single conformation. This precludes experiments to identify the endogenous tethered ligand binding site (LBS) and the conformational dynamics upon activation.

Amide hydrogen/deuterium exchange (H/D exchange) mass spectrometry (MS) is a structural approach that monitors the deuterium uptake at amide NH groups along the backbone of the protein by using MS.[17,18] The power of H/D exchange comes from comparing the deuterium uptake between 2 states to uncover the dynamics of ligand binding or receptor activation.[17-23] The distinct advantage of H/D exchange for G protein-coupled receptors (GPCRs) is that it overcomes the need for a stabilized receptor and allows us to examine the conformational dynamics of the tethered ligand mechanism.

Here, we describe the first biophysical studies of the PAR tethered ligand activation mechanism. We applied H/D exchange and computational modeling to uncover the endogenous LBS and a previously unknown function of extracellular loop 3 (ECL3). We verified the role of these regions with cell-based signaling assays. Taken together, we discovered a novel role of the ECL3 in PAR4 activation and demonstrated that the rigidity of this loop is critical to PAR4 activation. Finally, a polymorphism (rs2227376) that changes Pro to Leu in ECL3 significantly lowers PAR4 reactivity and is associated with a 15% reduction of relative risk of VTE.

Materials and methods

Protein expression and purification

Full-length human PAR4 containing an N-terminal FLAG tag was expressed and purified from *Sf9* cells as described previously.[24] The detailed purification protocols for both PAR4 and G-protein complex are described in the supplemental Data, available on the *Blood* Web site. The activity of purified PAR4 was verified as described in the supplemental Data.

Amide H/D exchange

Amide H/D exchange was performed and analyzed as described previously.[20,25] A detailed H/D exchange procedure, software list, and analysis pipeline are described in the supplemental Data. The H/D exchange was normalized to the maximal deuterium uptake at 10 minutes and the PAR4 homology model is color-coded as indicated in the legends for Figures 2 and 3. Gap regions are colored in gray. The difference map of the deuterium uptake level between nonactivated and thrombin activated contains only the peptides found in both states.

Computational modeling

The computational model of PAR4 in its thrombin-activated state was generated by using the crystal structure of rhodopsin at 2.2 Å resolution (Protein Data Bank entry 1U19) as described for green cone opsin.[20] The 2 sequences were aligned using the EMBOSS Needle Pairwise Sequence Alignment tool, and the initial model was generated using the MEDELLER server.[26,27] This initial model was imported into the ROSETTA protein structure prediction suite, and the loop building protocol was applied to determine the model with the lowest free energy. Additional details are provided in the supplemental Data.

Generation of PAR4-expressing cell lines

PAR4-wild-type (WT) or PAR4 mutants (PAR4-T153A, PAR4-T153S, PAR4-P310L, PAR4-S311A, and PAR4-P312L) containing an N-terminal V5 epitope were stably expressed using HEK293 Flp-In T-REx cells according to the manufacturer's protocol (Invitrogen). The concentration of tetracycline was titrated (25-1000 ng/mL) to yield similar expression levels of each PAR4 mutant on the cell surface (~175 000 receptors per cell) at 40 hours as determined by quantitative flow cytometry[28-30] (described in supplemental Data).

Measurement of intracellular calcium flux

PAR4-expressing HEK293 Flp-In T-REx cells were induced for 40 hours, removed from the plate and washed 3 times with *N*-2-hydroxyethylpiperazine-*N*′-2-ethanesulfonic acid (HEPES)-Tyrode's buffer (pH 7.4). Cells were incubated with 0.5 μM Fura-2 and 100 nM vorapaxar for 1 hour. The cells were then washed 3 times in HEPES-Tyrode's buffer with 200 μM $CaCl_2$ and diluted to 2.5×10^5 cells per mL. The intracellular calcium mobilization was recorded using a fluorometer (Photon Technology International, Inc.) for 420 seconds total. The first 50 seconds was set as the background, the response to agonist was measured for 250 seconds, and the maximum and minimum fluorescence was measured for 60 seconds each by adding 0.1% Triton X100 and 8.8 mM EDTA sequentially.[28,31,32] Fluorescence values were converted to intracellular free Ca^{2+} concentration with the equations described by Grynkiewicz et al.[31] A more detailed protocol is described in the supplemental Data.

Results

Analysis of PAR4 activation with H/D exchange

Full-length human PAR4 was expressed and purified in *Sf9* cells as described previously.[24] The protein was purified with affinity chromatography followed by size exclusion chromatography (Figure 1A). The purity of the protein was confirmed by both Coomassie staining and western blot analysis (Figure 1B). The dithiothreitol (DTT) in the purification procedure has the potential to affect the re-oxidation of the disulfide bond that connects ECL1 to ECL2 and influence the results of the H/D exchange. Therefore, we used a G-protein activation assay to confirm that the purified protein retains activity, which would indicate that the detergent and DTT present in the purification did not have an impact on protein folding (Figure 1C). The tandem mass spectrometry spectra of PAR4 digested by pepsin were analyzed by MassMatrix software. The peptide mapping studies had 91.2% (344 of 377) amino acid sequence coverage of the deuterated PAR4 (Figure 2A). The deuterium uptake of PAR4 ranged from 0% to 66%, which agrees with other GPCRs.[20,33,34]

The overall analysis identified conserved regions essential for GPCR signaling. As expected, the N- and C-termini had high deuterium uptake, indicating water accessibility; and the 7 transmembrane (TM) domains of PAR4 in both uncleaved (apo) state and activated state had limited deuterium uptake because they were being buried in detergent micelles (Figure 2B-G). Notably, TM4 and TM5 had less deuterium uptake compared with the other TM helices, suggesting that the dimerization interface of PAR4 was formed by TM4 and TM5 (supplemental Figure 1). This is in agreement with our previous biochemical studies, which also mapped the dimer interface to TM4, specifically to residues L192$^{4.41}$, L194$^{4.43}$, M198$^{4.47}$, and L202$^{4.51}$ (Ballesteros and Weinstein nomenclature).[29,30] Furthermore, the deuterium uptake at the dimer interface (M203$^{4.52}$-L213$^{4.62}$) decreased from 6.4% to 3.4% upon cleavage by thrombin, suggesting that the PAR4 dimer packed more tightly upon activation (supplemental Figure 1; supplemental Table 1). Intracellular loop 2 (ICL2) is the docking site for the heterotrimeric

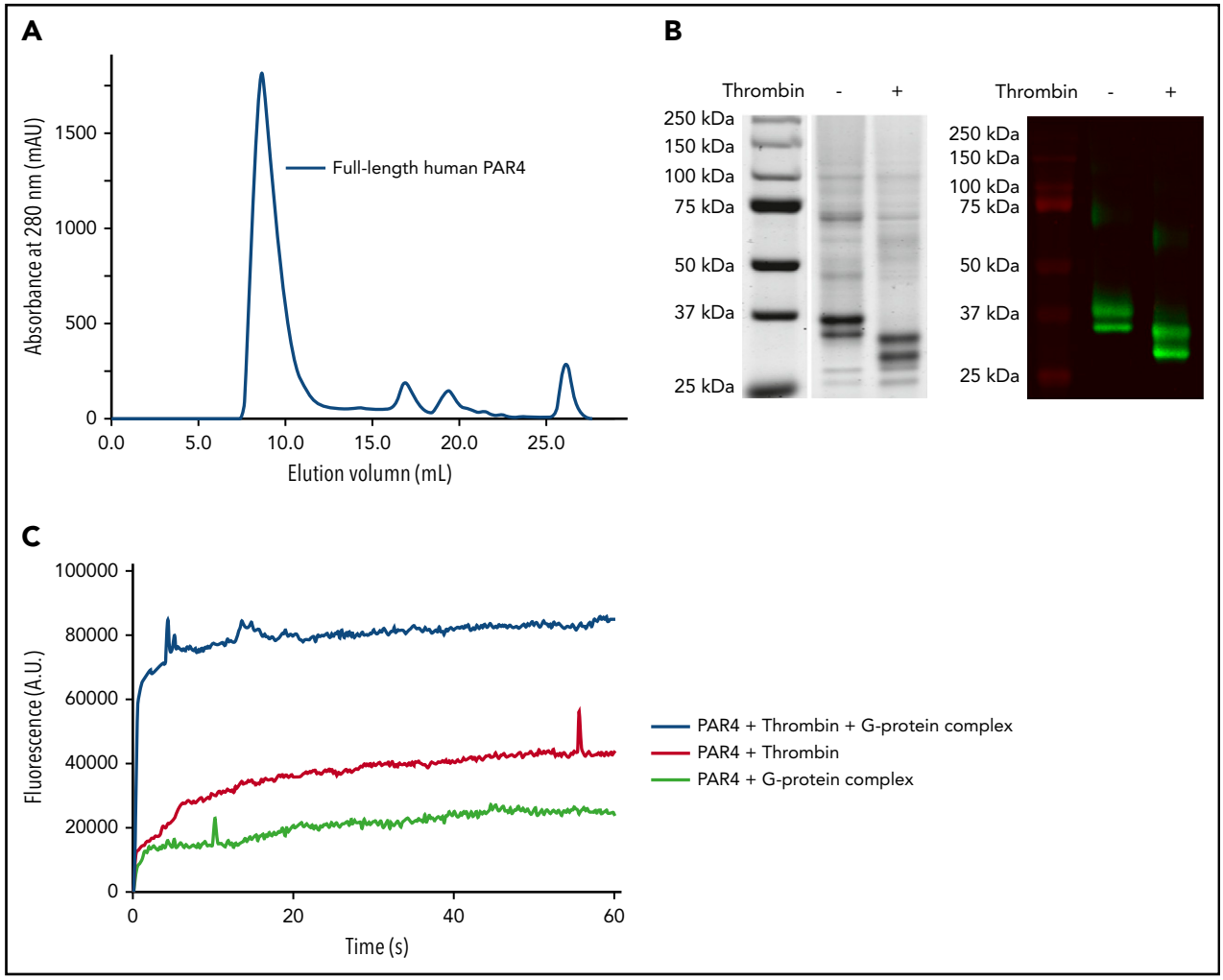

Figure 1. Human PAR4 expression and purification. Full-length human PAR4 was expressed and purified from *Sf9* cells. The protein was purified by FLAG antibody affinity chromatography followed by size exclusion chromatography. (A) A size exclusion chromatogram was obtained from purifications. Human PAR4 with a C-terminal 1D4 tag eluted in the main peak from fractions 14 to 20 (0.5 mL per fraction). The other small peaks contain tobacco etch virus for cutting the b562 RIL (BRIL) sequence from PAR4, the BRIL sequence, and the FLAG peptide for affinity chromatography. (B) Using both Coomassie staining (left) and immunoblotting with 1D4 antibody (right), the purity of the purified human PAR4 was confirmed. Purified PAR4 is a 37-kDa band on reduced sodium dodecyl sulfate-polyacrylamide gel electrophoresis with an extra glycosylated PAR4 band. The thrombin cleavage removed 2.9 kDa from the protein, and the activated PAR4 is at 34 kDa. (C) A G-protein assay measured the relative fluorescence change of tryptophan in the PAR4 and G-protein complex to confirm that the purified PAR4 is functional.

G-protein or arrestin and is essential for the propagation of intracellular signaling.[35-41] The H/D exchange of ICL2 (H180PLRA[184]) increased from 41% to 45% upon activation, which indicates that this loop had more solvent accessibility in the activated state (Figures 2B-G and 3; supplemental Table 1). These data suggest that ICL2 becomes accessible after receptor activation allowing the G-protein or arrestin to dock at its binding site. Helix 8 is a short α-helix between TM7 and the C terminus that may contribute to GPCR localization, receptor internalization, and/or G-protein activation.[42] The deuterium uptake in both apo and activated states was low (0.18%), indicating that it remains buried in the detergent (Figures 2B-G and 3; supplemental Table 1). However, the deuteration at the hinge region (amino acids Y[342] and VSAEF[347]) increased from 41% to 50%, showing that helix 8 is flexible in reference to the 7 transmembrane helical bundle (supplemental Table 1).

H/D exchange also identified novel regions unique to the tethered ligand mechanism of PAR4. On the basis of the current model of PAR activation, we predicted the N terminus would have a high deuterium uptake in the apo state that is reduced after the tethered ligand binds to a receptor. Surprisingly, in our H/D exchange studies, the PAR4 tethered ligand G[48]YPGQV had a low deuterium uptake in both apo and thrombin-activated states (Figures 2B-G and 3; supplemental Table 1), suggesting the tethered ligand docks near the extracellular loops before thrombin activation.

Comparing PAR4 in the apo and thrombin-activated states revealed 2 regions with a large change in deuteration upon activation (Figure 3). First, a region formed by amino acids C149[3.25]-L156[3.32] in TM3 and S329[7.42]-S333[7.46] in TM7 had significantly lower deuteration upon thrombin activation, suggesting that this is the LBS in which water accessibility was blocked by the tethered ligand upon proteolytic activation. Second, ECL3 and the adjacent regions of TM6 and TM7 (F296[6.48]-A327[7.40]) had increased deuterium uptake after thrombin activation (Figure 3). Given that this loop is located near the identified LBS, ECL3 may act as a

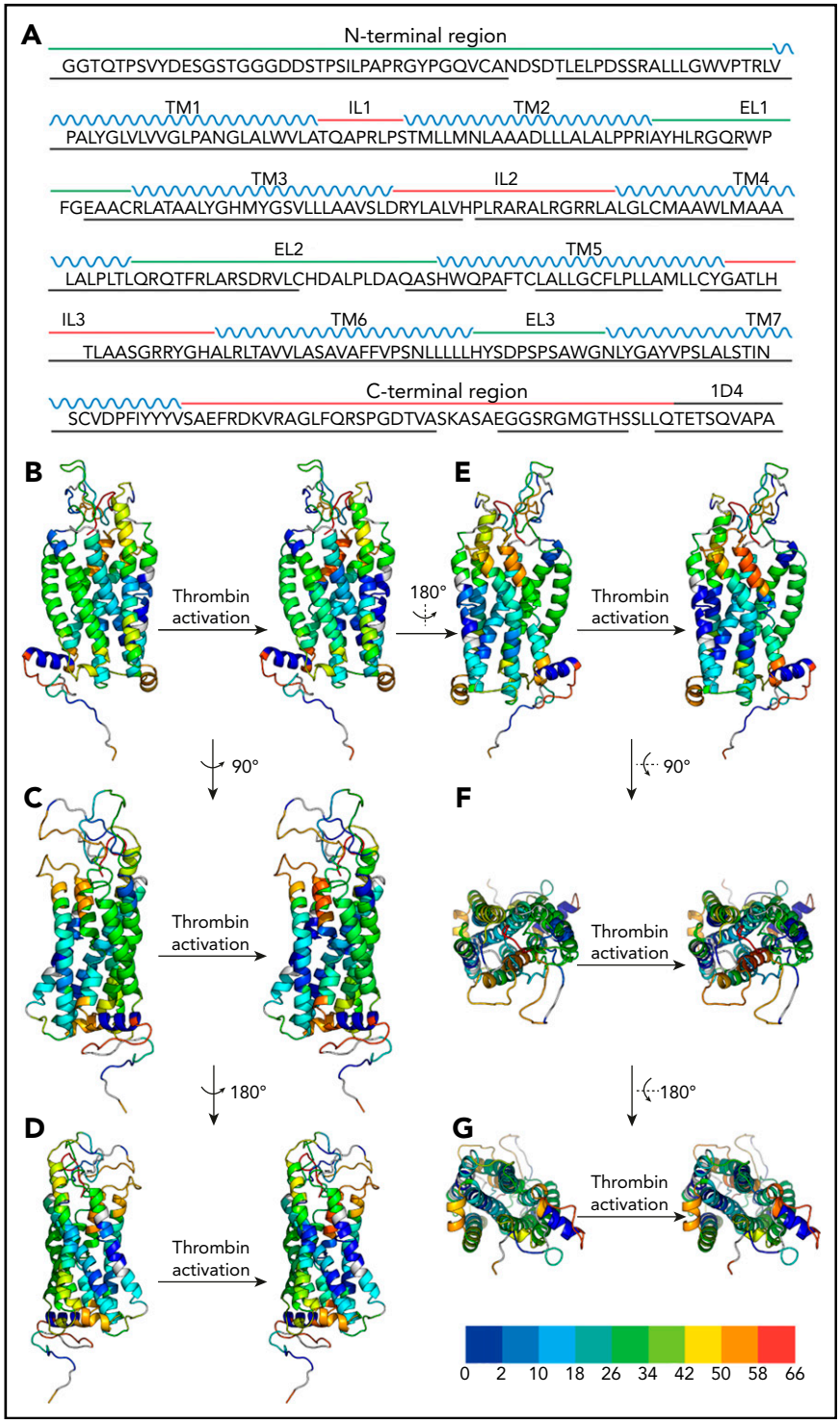

Figure 2. Peptide coverage of the human PAR4 construct by MS and H/D exchange map of the apo and thrombin-activated states of human PAR4. (A) Green line, the extracellular side of the PAR4 sequence; red line, the intracellular domain of PAR4; blue, the transmembrane domains; black, the C-terminal 1D4 tag. The black underline indicates the peptide coverage in H_2O, D_2O apo state, and D_2O thrombin-activated state. Only the peptides that are shown in all 3 states and that have a significant score with a *P* value <.05 were selected and further analyzed. (B-E) Side view of PAR4 in apo and thrombin-activated states. (F-G) Top and bottom views of PAR4 in apo and thrombin-activated states, respectively. In all panels, the apo state of PAR4 is on the left and the thrombin-activated state is on the right. The PAR4 homology model is color-coded on the basis of the H/D exchange level: dark blue for 0% to <2%, light blue for 2% to <10%, cyan for 10% to <18%, cadet blue for 18% to <26%, green for 26% to <34%, light green for 34% to <42%, yellow for 42% to <50%, orange for 5% to <58%, and red for 58% to 66%. Undefined regions are gray.

gatekeeper to prevent access of the tethered ligand to its binding site before thrombin activation of PAR4.

Computational modeling

To further validate the H/D exchange studies, a human PAR4 homology model in the thrombin-activated state was generated on the basis of the crystal structure of the prototypical Class A GPCR rhodopsin at a resolution of 2.2 Å.[20,43] The computational modeling was based on an original unbiased search of 10 000 computational models filtered by energetic allowance and optimized by searching for the energy landscape. The model with the lowest free energy level was selected. In this model, Gly48 in the tethered ligand interacts with Thr153 (Thr3.29) in the LBS identified in the H/D exchange studies (Figure 4). This raised the hypothesis that Thr153 has a critical role in PAR4 activation by forming a direct interaction with Gly48 from the tethered ligand upon thrombin activation.

Thr153 is critical for PAR4 ligand binding

H/D exchange and computational modeling suggested that Thr153 is critical for PAR4 activation. To test this in cells, we

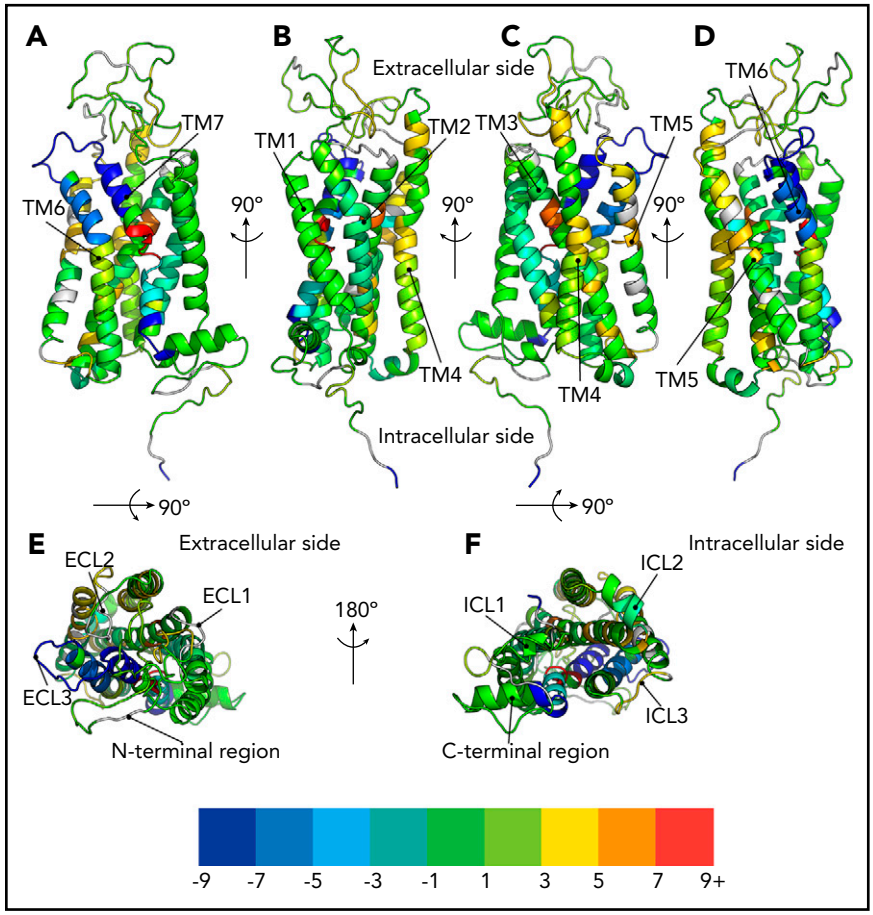

Figure 3. H/D exchange difference map of human PAR4 in apo and thrombin-activated states. The percent deuteration of the thrombin-activated state was subtracted from the percent deuteration of the apo state. The PAR4 homology model was color-coded on the basis of the difference in percent deuteration between the 2 states (Δ % deuteration [apo-activated]): dark blue for –9% to <−7%, light blue for −7% to <−5%, cyan for –5% to <−3%, cadet blue for –3% to <−1%, green for –1% to <1%, light green for 1% to <3%, yellow for 3% to <5%, orange for 5% to <7%, and red for 7% to 9+%. Undefined regions are gray. (A-D) Side views of PAR4. (E) Top view and (F) bottom view.

generated inducible cell lines stably expressing PAR4-WT, PAR4-T153A, or PAR4-T153S. To allow a direct comparison between each PAR4 mutant, the expression level of each construct was tuned by adjusting the tetracycline concentration to achieve ~175 000 receptors per cell as determined by quantitative flow cytometry (Figure 5A). Because HEK293 cells endogenously express PAR1, vorapaxar (100 nM) was used to block Ca^{2+} signaling from thrombin-activated PAR1 (supplemental Figure 2A-B); PAR1 inhibition was verified in all subsequent experiments (supplemental Figure 2C-N). We also confirmed that HEK293 cells do not respond to the PAR4-specific activation peptide (AYPGKF-NH_2) (supplemental Figure 2A).

Stimulation of PAR4-WT–expressing cells with 250 μM of the PAR4 activation peptide (AYPGKF-NH_2) led to a robust Ca^{2+} signal that was abolished by mutating Thr153 to Ala or Ser; a representative tracing is shown in Figure 5B. Furthermore, both PAR4-T153A and PAR4-T153S had a significant reduction of total Ca^{2+} flux as determined by area under the curve at all AYPGKF-NH_2 concentrations tested (30-1000 μM) (Figure 5C) and peak Ca^{2+} (supplemental Figure 3A). We next examined the response to the endogenous tethered ligand after activation by thrombin. There was a significant reduction in Ca^{2+} mobilization in PAR4-T153A–expressing cells when stimulated with 150 and 300 nM thrombin (Figure 5D; supplemental Figure 3B). PAR4-T153S had an intermediate response (Figure 5D; supplemental Figure 3B). These data show that mutating Thr153 reduced the response to both AYPGKF-NH_2 and thrombin but was less dramatic for thrombin. Taken together, Ca^{2+} signaling assays confirmed that Thr153 within the LBS identified by H/D exchange and predicted in the computational modeling is critical for PAR4 activation.

P310 on ECL3 of PAR4 is important for receptor activation

ECL3 had increased deuteration after thrombin activation, which indicates that it becomes exposed to solvent (Figure 3). On the basis of the location of this loop relative to the PAR4 LBS, we hypothesized that it acts as a gatekeeper that swings out after activation by thrombin, which allows the tethered ligand to access the binding pocket. The computational modeling of thrombin-activated PAR4 demonstrated that ECL3 adopts in an "out" position further supporting the gatekeeper hypothesis (supplemental Movie 1). Eight of the 10 residues in ECL3 are identical among human, mouse, and rat PAR4, which suggests a conserved function between species (supplemental Figure 4). Notably, there are 2 proline residues located in ECL3. Prolines located in loops often have a critical role in maintaining the rigidity of these regions.[44] Therefore, we postulated that Pro310 and Pro312 are important for maintaining the loop rigidity for PAR4 activation.

We have previously shown that naturally occurring variants in human PAR4 alter receptor reactivity and affect platelet function.[13] Coincidently, there is an uncharacterized polymorphism of PAR4 (rs2227376) that changes proline to leucine at position 310 (P310L) in ECL3. We postulated that substituting a leucine for proline in ECL3 would lead to increased flexibility and affect

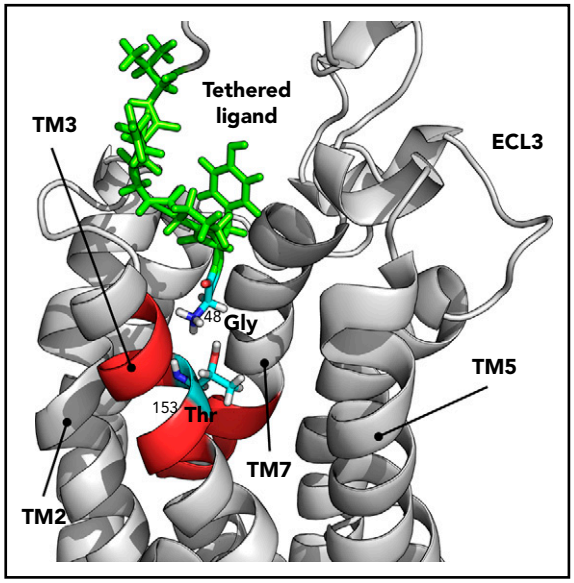

Figure 4. Structural modeling showing the interaction between the tethered ligand and the LBS. The homology model for PAR4 in the activated state was generated by computational modeling. In this model, the tethered ligand is green, the LBS is red, and Gly48 and Thr153 are cyan. The TM4 and part of ECL2 are hidden on the homology model to provide a better view of the LBS.

the structural integrity of ECL3, which would have an impact on PAR4 activation and signaling. To test this experimentally, we generated a stable cell line expressing PAR4-P310L (Figure 6A). Mutating Pro310 to Leu abolished total Ca^{2+} signaling in response to the AYPGKF-NH_2 peptide as determined by AUC (Figure 6B-C) and peak Ca^{2+} (supplemental Figure 5A). The response to thrombin was also significantly reduced (Figure 6D; supplemental Figure 5B). Next, we determined whether other residues in ECL3 contribute to PAR4 function. Pro310 is found within a conserved sequence (P310SP) (supplemental Figure 4). We generated PAR4-S311A, which is predicted to have no impact on the rigidity of ECL3, and PAR4-P312L, which is predicted to increase the flexibility of ECL3. Mutating Ser311 to Ala did not impact Ca^{2+} signaling in response to AYPGKF-NH_2 or thrombin (Figure 6B-D; supplemental Figure 5). Interestingly, mutated Pro312 had an intermediate response to AYPGKF-NH_2 compared with PAR4-WT and PAR4-P310L (Figure 6B-C; supplemental Figure 5A). PAR4-P312L seemed to be hyperreactive in response to thrombin, but it did not reach statistical significance (Figure 6D; supplemental Figure 5B). Taken together, these data indicate that the intact rigidity of ECL3 is essential for PAR4 activation.

PAR4-310L allele correlates with a reduced risk of VTE

PAR4 single nucleotide polymorphisms (SNPs) are known to have an impact on platelet function.[13] Recently, it was recognized that platelets have a role in the initiation of venous thrombosis, so we examined the correlation of rs2227376 (PAR4-310P/L) and rs773902 (PAR4-120A/T) with VTE. The International Network Against Venous Thrombosis (INVENT) Consortium is a multi-ancestry genome-wide association study meta-analysis with 30 234 VTE cases and 172 122 controls and has been used to identify novel genetic markers for VTE.[45] The minor allele frequency for rs2227376 was 0.015 for individuals with European ancestry, and this polymorphism was not present in participants with African ancestry. The PAR4 allele encoding for Leu at 310 had a 15% reduction in relative risk for VTE (odds ratio, 0.85; 95% confidence interval, 0.77-0.94) compared with the Pro for each Leu allele. Protection from VTE is consistent with the Leu having decreased PAR4 reactivity. The minor allele frequency for rs773902 was 0.19 in those with European ancestry and 0.45 in those with African ancestry, which is consistent with previous reports. However, rs773902 was not associated with VTE in the INVENT data: odds ratio, 1.02; 95% confidence interval, 0.99-1.05).

Discussion

PARs are important mediators that facilitate communication between proteases and the intracellular signaling machinery. Since PARs were discovered, their roles in a wide range of processes have been intensely studied and are well characterized.[4-9,46-49] However, the biophysical and structural basis for the activation mechanism of this receptor family is still limited. In addition, the location of the tethered LBS of PAR is unclear. Here, we applied amide H/D exchange MS combined with computational modeling and cell signaling to uncover the location of the endogenous LBS and the structural basis for the tethered ligand–mediated activation mechanism for PAR4.

We and others have previously shown that PAR4 forms homodimers and heterodimers with PAR1, PAR3, and P2Y12.[29,30,50-55] These physical interactions have an impact on receptor activation, signaling, and response to antagonists. We observed less deuterium uptake in TM4 and TM5 compared with the other helices. The tight packing arrangement of this region suggests a homodimer interface (supplemental Figure 1). Consistent with these data, we previously mapped the PAR4 homodimer interface to TM4 using biochemical and signaling studies.[30] The heterodimer interface of PAR4 with PAR1 and P2Y12 have also been mapped to TM4.[29,50] The agreement of our H/D exchange data with published studies of PARs and other GPCRs gives us confidence that our recombinant protein accurately represents PAR4 expressed on cells.[51,56-59]

The precise nature of the interactions between the tethered ligand and the receptor has remained elusive. Initial studies with PAR1 and PAR2 revealed a role for ECL2.[10,60,61] Nanevicz et al[10] showed a complementary relationship between ECL2 and the tethered ligand in elegant studies using a panel of human-*Xenopus* PAR1 chimeric receptors.[10,60] Mutagenesis studies have also identified key residues in ECL2 for PAR2.[61] Our H/D exchange difference map identified a binding pocket formed by TM3 and TM7 on the extracellular side of the receptor that had significantly less deuterium uptake in the thrombin-activated PAR4. This suggests that the tethered ligand blocked solvent accessibility to this region (Figure 3). In addition, ECL3 had increased deuterium uptake after activation, which indicated an increase in solvent accessibility of this loop. Computational modeling confirmed the H/D exchange showing that Gly48 of the tethered ligand interacts with Thr153 in the binding pocket and that ECL3 is in an open conformation (Figure 4). These data support a unique mechanism for PAR4 activation by the tethered ligand that involves a deep binding pocket within the TM helices and ECL3, which has not been identified for PAR1 and PAR2. PAR4 has signaling characteristics distinct from those of PAR1 and PAR2. PAR4 mediates prolonged signaling in platelets and

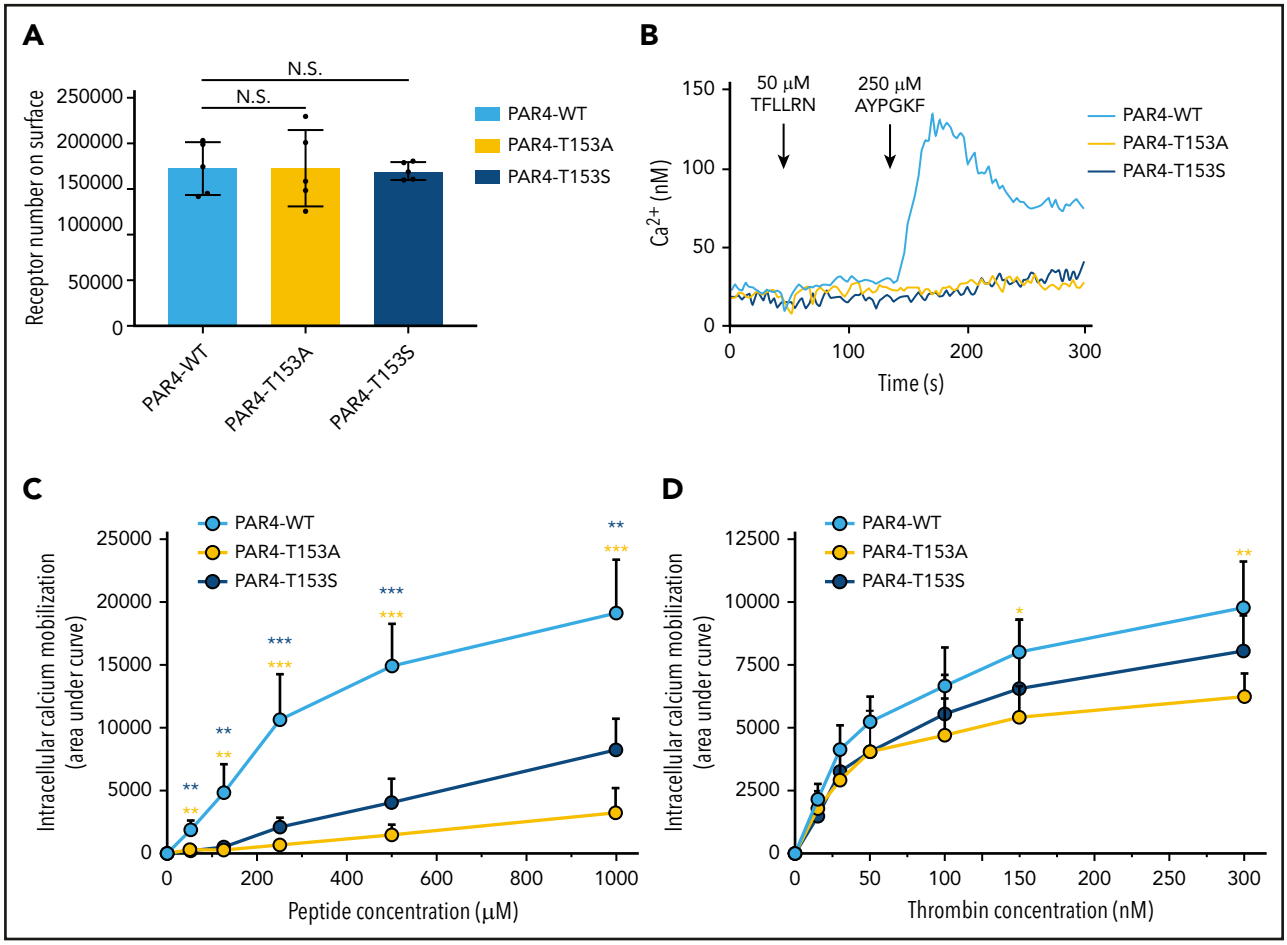

Figure 5. Thr153 in the LBS is critical for PAR4 activation. (A) Comparable expression levels of PAR4-WT, PAR4-T153A, and PAR4-T153S on the surface of the HEK293 Flp-In T-REx stable cell lines confirmed by flow cytometry using a V5-fluorescein isothiocyanate (FITC)–conjugated antibody. (B) HEK293 cell expresses PAR1 endogenously, which is inhibited by 100 nM vorapaxar. There is no intracellular calcium mobilization triggered by stimulating HEK293 Flp-In T-REx cells that express PAR4-WT, PAR4-T153A, or PAR4-T153S with 50 μM PAR1-AP (TFLLRN). Stimulating PAR4-WT with 250 μM of PAR4-AP initiated calcium flux, but PAR4-T153A and PAR4-T153S had no response to this dose of PAR4-AP. (C) PAR4-WT, PAR4-T153A, and PAR4-T153S were challenged with 5 different doses of PAR4-AP, and calcium mobilization responses to PAR4-AP stimulation were measured (n = 5). Data are presented as the area under curve (AUC) after stimulation of the Fura2-loaded HEK293 Flp-In T-REx stable cell lines. (D) PAR4-WT, PAR4-T153A, and PAR4-T153S were challenged with 6 different doses of α-thrombin, and calcium mobilization responses to α-thrombin stimulation were measured (n = 5). Data are presented as the AUC after stimulation of the Fura2-loaded HEK293 Flp-In T-REx stable cell lines. Data are mean ± standard deviation (SD) from 5 independent experiments at each concentration. N.S., not significant, unpaired Student *t* test. *$P < .05$; **$P < .01$; ***$P < .001$. The yellow asterisks indicate the comparison of PAR4-T153A to PAR4-WT and the blue asterisks indicate the comparison of PAR4-T153S to PAR4-WT.

other cells.[11,62,63] In contrast, PAR1 and PAR2 mediate transient signaling.[61-63] We propose that the deep binding pocket we identified may contribute to the sustained signaling of PAR4, whereas the transient signaling of PAR1 and PAR2 may be mediated by transient interactions with ECL2 on the surface of the receptor. Our H/D exchange and modeling did not reveal a role for ECL2. However, a recent study by Thibeault et al[64] showed that His229 and Asp230 in ECL2 are critical for PAR4 activation. This discrepancy may be a result of interactions between the exodomain and extracellular loops before activation that prevent H/D exchange. Traditionally, the N terminus of PARs is thought to be unstructured and highly flexible. Therefore, we hypothesized that it would have high deuterium uptake in the apo state that decreased upon activation by the protease. Unexpectedly, the PAR4 exodomain including the tethered ligand (^{48}GYPGQV) had low deuterium uptake in both states, suggesting that the N terminus of PAR4 docks near the extracellular loops before activation. These interactions may limit H/D exchange at ECL2 and the exodomain. Histidine H/D exchange allows analysis of site specific changes in protein structure using the imidazole C2-hydrogen on the histidine residue as a probe.[65-67] Our histidine H/D exchange analysis of PAR4 showed a twofold increase in the $t_{1/2}$ for H/D exchange at His229 in thrombin-activated PAR4, which supports a role for ECL2 in PAR4 activation.[24] Taken together, these data suggest a more complex arrangement on the extracellular face of PAR4, which can also potentially have an impact on the interactions between PAR4 and thrombin. The conventional model is that proteases interact solely with exodomains of PARs.[8,9,14,68,69] Sánchez Centellas et al[70] reported that an anionic cluster (Asp224, Asp230, Asp235) in ECL2 is important for PAR4 activation by thrombin, which agrees with a more complex model of PAR4 activation that has emerged with roles for the extracellular loops of the PAR4 and exosite II of thrombin.[70-72] Our model in which the N terminus is docked near the extracellular loops would facilitate these additional interactions between PAR4 and thrombin.

The H/D exchange and molecular modeling identified 2 regions of PAR4 that may be important for activation: Thr153 in the LBS

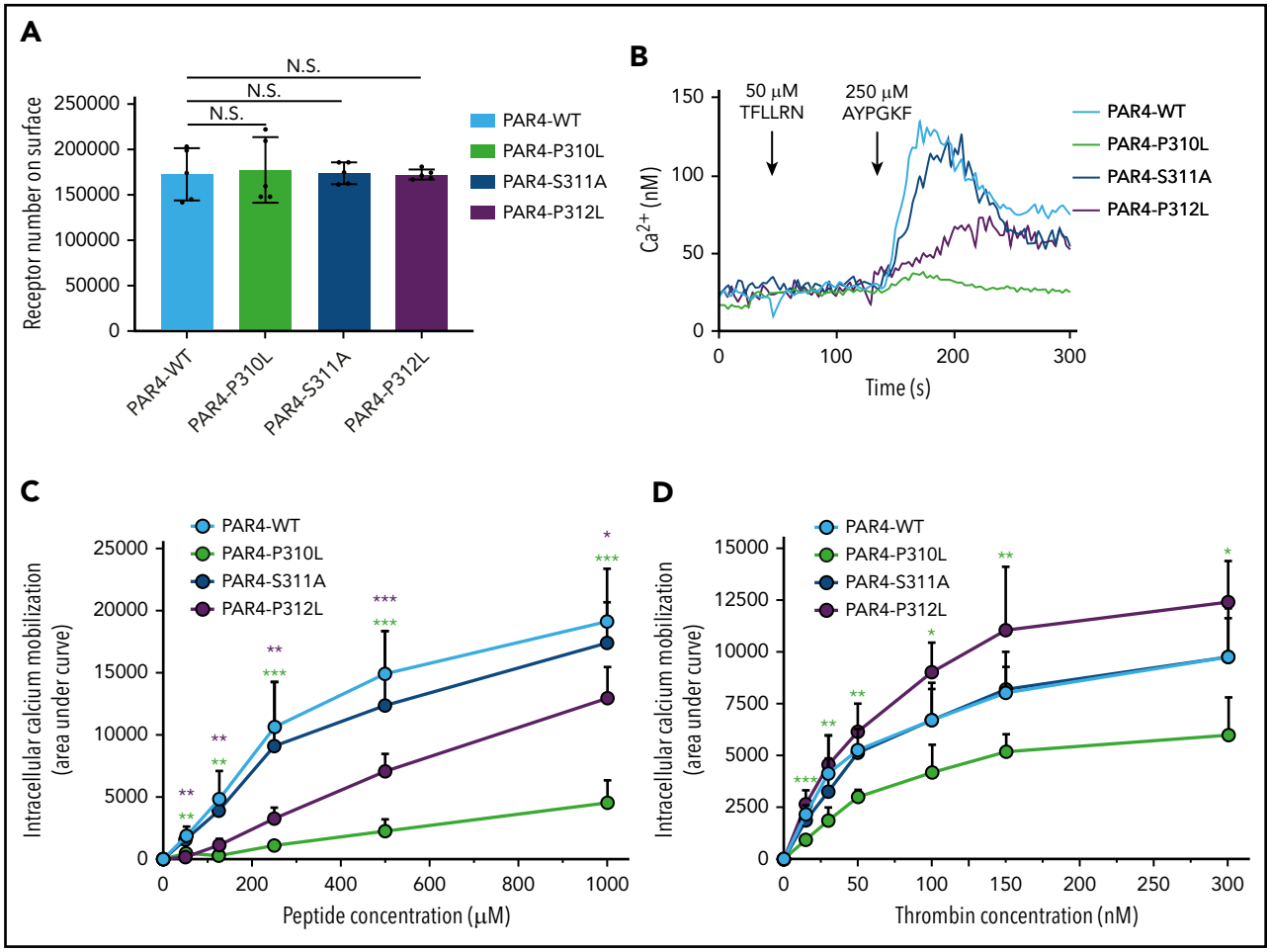

Figure 6. The intact rigidity of ECL3 is essential for the interaction between the tethered ligand and the binding site. (A) Comparable expression levels of PAR4-WT, PAR4-P310L, PAR4-S311A, and PAR4-P312L on the surface of the HEK293 Flp-In T-REx stable cell lines were confirmed by flow cytometry using a V5-FITC–conjugated antibody. (B) Endogenous PAR1 in HEK293 cells is inhibited by 100 nM vorapaxar. No intracellular calcium mobilization was triggered by stimulating HEK293 Flp-In T-REx cells that express PAR4-WT, PAR4-P310L, PAR4-S311A, and PAR4-P312L with 50 μM PAR1-AP. Stimulating PAR4-WT with 250 μM of PAR4-AP initiated calcium flux, and PAR4-P310L had a small but unmistakable response to the same dose of PAR4-AP. At this dose of PAR4-AP, PAR4-S311A cells showed a receptor reactivity similar to that of PAR4-WT, and PAR4-P312L had a hyporesponse to PAR4-AP stimulation. (C) PAR4-WT, PAR4-P310L, PAR4-S311A, and PAR4-P312L were challenged with 5 different doses of PAR4-AP, and calcium mobilization responses to PAR4-AP stimulation were measured (n = 5). Data are presented as the AUC after stimulation of the Fura2-loaded HEK293 Flp-In T-REx stable cell lines. (D) PAR4-WT, PAR4-P310L, PAR4-S311A, and PAR4-P312L were challenged with 6 different doses of α-thrombin, and calcium mobilization responses to thrombin stimulation were measured (n = 5). Data are presented as the AUC after stimulation of the Fura2-loaded HEK293 Flp-In T-REx stable cell lines. Data are mean ± SD from 5 independent experiments at each concentration. Unpaired Student *t* test; **P* < .05; ***P* < .01; ****P* < .001.

and ECL3. Mutating Thr153 to Ala reduced PAR4-mediated Ca^{2+} signaling. The more conserved substitution to Ser also led to a decrease in Ca^{2+} mobilization, albeit to a lesser extent (Figure 5; supplemental Figure 3). Taken together, these data demonstrate that both the size and polarity of Thr153 in the LBS are critical for PAR4 signaling. ECL3 had increased H/D exchange in the thrombin-activated PAR4 and adopted an outward confirmation in the computational model. This led us to propose that ECL3 serves as a gatekeeper to block the interaction between the N terminus and the LBS before enzymatic cleavage (Figure 7). In this model, ECL3 swings outward to allow the tethered ligand access to the LBS. We propose a coordinated movement of ECL3 that is facilitated by its rigidity conferred by 2 conserved prolines: Pro310 and Pro312 (Figure 6; supplemental Figure 5).[44,73] Mutating either of these residues had an impact on PAR4 signaling, whereas mutating Ser311, which is not predicted to influence loop rigidity, had no effect on signaling. In other studies, mutating Asp309 did not have an impact on signaling, which gives further support to the role of the prolines and loop rigidity.[70]

We observed that PAR4 mutations had greater impact on signaling initiated by PAR4 activating peptide (PAR4-AP) compared with thrombin (Figures 5 and 6). The simple explanation is that the tethered ligand cannot diffuse, which makes it readily available to re-associate with the receptor once the ligand dissociates; this minimizes the impact of the PAR4 mutations. Alternatively, the activation peptides may have distinct interactions and consequences of binding to the receptors. We have recently shown that thrombin-activated PAR4 is resistant to proteolysis by thermolysin, whereas PAR4-AP-stimulated PAR4 had the same digestion profile as unstimulated PAR4.[24] These data strongly suggest that the overall conformation is different for the receptor when it is activated by the tethered ligand. Furthermore, signaling initiated by PAR activation peptides is not identical to protease activation of PARs.[64,74] Thibeault et al[64]

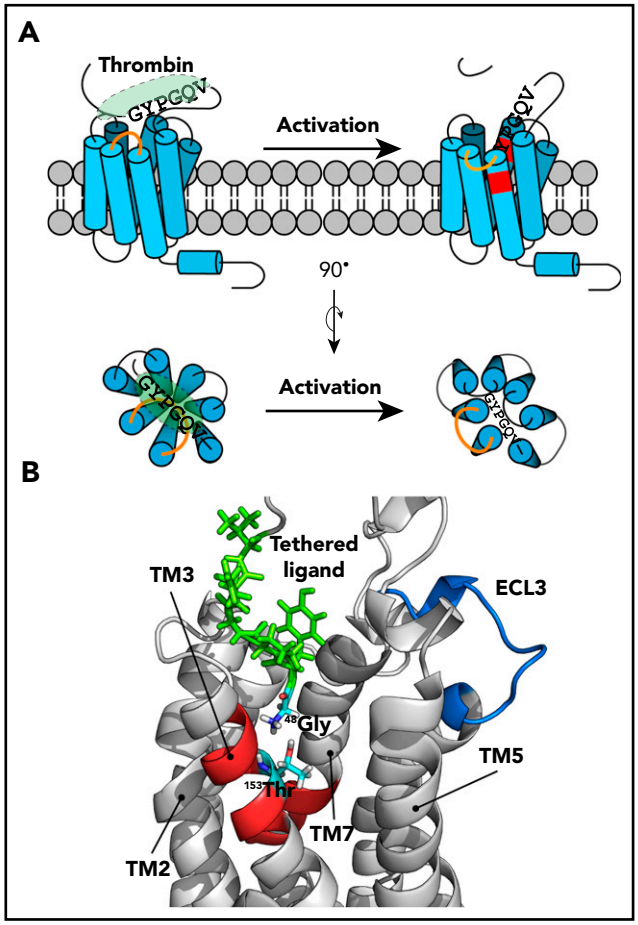

Figure 7. Tethered ligand–mediated PAR4 activation model. (A) Before thrombin activation, the tethered ligand is buried and already docks close to the LBS of PAR4. The interaction between the tethered ligand and its binding site is blocked by ECL3 (orange line). Thrombin cleavage triggers a structural rearrangement of ECL3 that opens the accessibility between the tethered ligand and the binding site. The tethered ligand drops directly into the LBS (shown in red) and the Gly48 interacts with Thr153 to further initiate downstream signaling, which requires G-protein complex to recruit and dock at ICL2 of PAR4. (B) The computational modeling of the thrombin-activated PAR4 model, in which the ECL3 adapted in an "out" position to provide space for the tethered ligand to interact with the binding site further support the working model of the PAR4 activation mechanism. The tethered ligand is green, the LBS is red, and the ECL3 is blue.

recently used an extensive panel of activation peptides to analyze biased signaling from PAR4. They identified specific residues in the PAR4-AP that activated G_q signaling that were distinct from those that activated arrestin signaling. To date, there have been no reports of biased signaling resulting from protease activation of endogenous PAR4. However, Thibeault et al[64] and Ramachandran et al[75] have shown the capacity of PAR4 to elicit biased signaling. In our studies, we used Ca^{2+} signaling as a readout of receptor function to validate our H/D exchange and modeling. Going forward, it will be necessary to determine how the regions we identified influence additional signaling pathways downstream of PAR4. In particular, it will be important to determine how the naturally occurring variant PAR4-P310L influences platelet activation via each of these pathways as well as crosstalk with other GPCRs such as P2Y12.[50,53,76]

A common SNP leads to PAR4 sequence variants at position 120 (Thr or Ala) in TM2 (rs773902). A Thr at this position results in a hyperreactive PAR4 compared with an Ala.[13,77,78] To date, the mechanism for this functional difference has not been described, and it is unclear how changing an amino acid in TM2 impacts PAR4 reactivity. Interestingly, Thr120 is near the region we identified as the LBS (supplemental Figure 6). This raises the intriguing possibility that the Thr or Ala at 120 is close enough to the LBS to have an impact on how the tethered ligand interacts with this region. In this study, we also describe the first functional consequences of PAR4 variants at 310 (Pro or Leu) resulting from rs2227376 and directly demonstrate a role for ECL3 and Pro310 in PAR4 activation.

Venous thrombosis and its major complication pulmonary embolism is called VTE and is a major cause of morbidity and mortality.[79] Hypercoagulation, stasis, and endothelial dysfunction (Virchow's triad) are the primary drivers of VTE. Platelets also have an essential initiating role, but the mechanisms are poorly understood.[2] Given that PAR4 promotes procoagulant platelets, phosphatidyl serine exposure, and subsequent thrombin generation, it is a potential contributor to VTE.[80-82] We evaluated the correlation of 2 PAR4 SNPs, rs773902 and rs2227376, with risk of VTE by using the INVENT Consortium resources.[45] Interestingly, PAR4-120A/T (rs773902) was not associated with VTE, whereas the hyporeactive PAR4-310L (rs2227376) was associated with a 15% reduction in relative risk. The differences between these polymorphisms is likely related to their impact on PAR4 reactivity. PAR4-120A has a higher concentration of drug that gives half-maximal response (EC_{50}) than PAR4-120T; however, the maximum signaling for these is the same. In contrast, PAR4-310L has a reduced response to low thrombin concentrations and a lower maximum reactivity, which likely leads to the protection from VTE. The data suggest a previously unrecognized role for PAR4 in the pathology of VTE. Going forward, mechanistic studies are required to determine how PAR4 on platelets and other cells contributes to the initiation and propagation of VTE.

PARs have become promising therapeutic targets.[48,83,84] Competing with the tethered ligand creates unique challenges to developing therapeutic agents with favorable pharmacologic profiles. There has been progress with PAR4, but the lack of studies that directly determine the binding site for the endogenous tethered ligand has slowed efforts to development new drugs.[12,85] Therefore, high-resolution structure of full-length PAR4 in its natural lipid environment without sequence modifications will greatly facilitate drug discovery. Future studies on PAR4 that combine amide-H/D exchange with recent technological breakthroughs in cryo electron microscopy will untangle the questions raised in our studies. First, a high-resolution structure of activated PAR4 will determine whether Thr153 directly interacts with the tethered ligand or if it merely influences the size and shape of the binding pocket. Second, these will also determine the structural basis for how each SNP contributes to PAR4 function. Third, determining the structure of PAR4 in complex with thrombin will reveal the contributions of ECL2 and ECL3. Fourth, structures of PAR4 signaling complexes in their natural lipid environment will elucidate the mechanism of dimer-mediated signaling.[86,87]

In conclusion, our findings provide the first description of the PAR tethered ligand activation mechanism. By using H/D exchange, we identified the endogenous tethered LBS and a role for ECL3 in PAR4 activation. We also identified a functional

consequence of a PAR4 SNP in ECL3 that leads to a 15% reduction in relative risk of VTE. These studies point to a role for PAR4 in the development of VTE.

Acknowledgments

The authors thank Tivadar Orban for helpful discussions on H/D exchange and critical reading of the manuscript and Nicholas L. Smith for critical reading of the INVENT data.

This study was supported by a grant from the National Institutes of Health (NIH) National Heart Lung and Blood Institute (NHLBI) (HL098217) (M.T.N.) and the American Heart Association (15GRNT25090222) (M.T.N.). X.H. received research funding from the American Heart Association 2018 Predoctoral Fellowship (18PRE33960396) and is cofunded by the Schwab Charitable Fund. This research was supported in part by grant R24EY027283 to K.P. from the NIH National Eye Institute and the Immune Core Facility in the CWRU/UH Center for AIDS Research (NIH grant: P30 AI036219). The authors also acknowledge support from an RPB unrestricted grant to the Department of Ophthalmology, University of California, Irvine. The INVENT Consortium is supported in part by NIH, NHLBI grant HL134894.

Authorship

Contribution: X.H., K.P., and M.T.N. conceived the study; X.H., L.H., M.d.l.F., and M.T.N. designed the experiments; X.H., M.d.l.F., N.A., and M.T.N. performed the experiments and analyzed the data; X.H. and M.T.N. wrote the manuscript; and M.d.l.F., L.H., N.A., and K.P. critically read and edited the manuscript.

Conflict-of-interest disclosure: The authors declare no competing financial interests.

A complete list of the members of the INVENT Consortium appears in the supplemental appendix.

ORCID profiles: X.H., 0000-0002-1977-1046; L.H., 0000-0003-0157-0526; M.d.l.F., 0000-0002-0249-9728; M.T.N., 0000-0003-2602-023X.

Correspondence: Marvin T. Nieman, Department of Pharmacology, Case Western Reserve University, 2109 Adelbert Rd, Wood Building, W309B, Cleveland, OH 44106-4965; e-mail: nieman@case.edu.

Footnotes

Submitted 27 December 2019; accepted 24 May 2020; prepublished online on *Blood* First Edition 23 June 2020. DOI 10.1182/blood.2019004634.

Original data is available by e-mailing the corresponding author.

The online version of this article contains a data supplement.

There is a *Blood* Commentary on this article in this issue.

The publication costs of this article were defrayed in part by page charge payment. Therefore, and solely to indicate this fact, this article is hereby marked "advertisement" in accordance with 18 USC section 1734.

REFERENCES

1. Foley JH, Conway EM. Cross talk pathways between coagulation and inflammation. *Circ Res*. 2016;118(9):1392-1408.
2. Rodrigues SF, Granger DN. Blood cells and endothelial barrier function. *Tissue Barriers*. 2015;3(1-2):e978720.
3. Heuberger DM, Schuepbach RA. Protease-activated receptors (PARs): mechanisms of action and potential therapeutic modulators in PAR-driven inflammatory diseases. *Thromb J*. 2019;17(1):4.
4. Vu TK, Hung DT, Wheaton VI, Coughlin SR. Molecular cloning of a functional thrombin receptor reveals a novel proteolytic mechanism of receptor activation. *Cell*. 1991;64(6):1057-1068.
5. Ishihara H, Connolly AJ, Zeng D, et al. Protease-activated receptor 3 is a second thrombin receptor in humans. *Nature*. 1997;386(6624):502-506.
6. Nystedt S, Emilsson K, Larsson AK, Strömbeck B, Sundelin J. Molecular cloning and functional expression of the gene encoding the human proteinase-activated receptor 2. *Eur J Biochem*. 1995;232(1):84-89.
7. Nystedt S, Emilsson K, Wahlestedt C, Sundelin J. Molecular cloning of a potential proteinase activated receptor. *Proc Natl Acad Sci U S A*. 1994;91(20):9208-9212.
8. Xu WF, Andersen H, Whitmore TE, et al. Cloning and characterization of human protease-activated receptor 4. *Proc Natl Acad Sci U S A*. 1998;95(12):6642-6646.
9. Nieman MT. Protease-activated receptors in hemostasis. *Blood*. 2016;128(2):169-177.
10. Nanevicz T, Ishii M, Wang L, et al. Mechanisms of thrombin receptor agonist specificity. Chimeric receptors and complementary mutations identify an agonist recognition site. *J Biol Chem*. 1995;270(37):21619-21625.
11. Kahn ML, Nakanishi-Matsui M, Shapiro MJ, Ishihara H, Coughlin SR. Protease-activated receptors 1 and 4 mediate activation of human platelets by thrombin. *J Clin Invest*. 1999;103(6):879-887.
12. Wong PC, Seiffert D, Bird JE, et al. Blockade of protease-activated receptor-4 (PAR4) provides robust antithrombotic activity with low bleeding. *Sci Transl Med*. 2017;9(371):eaaf5294.
13. Edelstein LC, Simon LM, Lindsay CR, et al. Common variants in the human platelet PAR4 thrombin receptor alter platelet function and differ by race. *Blood*. 2014;124(23):3450-3458.
14. Seeley S, Covic L, Jacques SL, Sudmeier J, Baleja JD, Kuliopulos A. Structural basis for thrombin activation of a protease-activated receptor: inhibition of intramolecular liganding. *Chem Biol*. 2003;10(11):1033-1041.
15. Zhang C, Srinivasan Y, Arlow DH, et al. High-resolution crystal structure of human protease-activated receptor 1. *Nature*. 2012;492(7429):387-392.
16. Cheng RKY, Fiez-Vandal C, Schlenker O, et al. Structural insight into allosteric modulation of protease-activated receptor 2. *Nature*. 2017;545(7652):112-115.
17. Bai Y, Milne JS, Mayne L, Englander SW. Primary structure effects on peptide group hydrogen exchange. *Proteins*. 1993;17(1):75-86.
18. Liepinsh E, Otting G. Proton exchange rates from amino acid side chains–implications for image contrast. *Magn Reson Med*. 1996;35(1):30-42.
19. Gallagher ES, Hudgens JW. Mapping protein-ligand interactions with proteolytic fragmentation, hydrogen/deuterium exchange-mass spectrometry. *Methods Enzymol*. 2016;566:357-404.
20. Hofmann L, Alexander NS, Sun W, Zhang J, Orban T, Palczewski K. Hydrogen/deuterium exchange mass spectrometry of human green opsin reveals a conserved pro-pro motif in extracellular loop 2 of monostable visual G protein-coupled receptors. *Biochemistry*. 2017;56(17):2338-2348.
21. Katta V, Chait BT. Conformational changes in proteins probed by hydrogen-exchange electrospray-ionization mass spectrometry. *Rapid Commun Mass Spectrom*. 1991;5(4):214-217.
22. Malito E, Faleri A, Lo Surdo P, et al. Defining a protective epitope on factor H binding protein, a key meningococcal virulence factor and vaccine antigen. *Proc Natl Acad Sci U S A*. 2013;110(9):3304-3309.
23. Zhang Z, Smith DL. Determination of amide hydrogen exchange by mass spectrometry: a new tool for protein structure elucidation. *Protein Sci*. 1993;2(4):522-531.
24. de la Fuente M, Han X, Miyagi M, Nieman MT. Expression and purification of protease-activated receptor 4 (PAR4) and analysis with histidine hydrogen-deuterium exchange. *Biochemistry*. 2020;59(5):671-681.
25. Xu H, Freitas MA. Automated diagnosis of LC-MS/MS performance. *Bioinformatics*. 2009;25(10):1341-1343.
26. Rice P, Longden I, Bleasby A. EMBOSS: the European Molecular Biology Open Software Suite. *Trends Genet*. 2000;16(6):276-277.
27. Kelm S, Shi J, Deane CM. MEDELLER: homology-based coordinate generation for

membrane proteins. *Bioinformatics*. 2010; 26(22):2833-2840.

28. Arachiche A, de la Fuente M, Nieman MT. Platelet specific promoters are insufficient to express protease activated receptor 1 (PAR1) transgene in mouse platelets. *PLoS One*. 2014;9(5):e97724.

29. Arachiche A, Mumaw MM, de la Fuente M, Nieman MT. Protease-activated receptor 1 (PAR1) and PAR4 heterodimers are required for PAR1-enhanced cleavage of PAR4 by α-thrombin. *J Biol Chem*. 2013;288(45): 32553-32562.

30. de la Fuente M, Noble DN, Verma S, Nieman MT. Mapping human protease-activated receptor 4 (PAR4) homodimer interface to transmembrane helix 4. *J Biol Chem*. 2012; 287(13):10414-10423.

31. Grynkiewicz G, Poenie M, Tsien RY. A new generation of Ca2+ indicators with greatly improved fluorescence properties. *J Biol Chem*. 1985;260(6):3440-3450.

32. Arachiche A, de la Fuente M, Nieman MT. Calcium mobilization and protein kinase C activation downstream of protease activated receptor 4 (PAR4) is negatively regulated by PAR3 in mouse platelets. *PLoS One*. 2013;8(2): e55740.

33. Zhang X, Chien EY, Chalmers MJ, et al. Dynamics of the beta2-adrenergic G-protein coupled receptor revealed by hydrogen-deuterium exchange. *Anal Chem*. 2010;82(3): 1100-1108.

34. Duc NM, Du Y, Zhang C, et al. Effective application of bicelles for conformational analysis of G protein-coupled receptors by hydrogen/deuterium exchange mass spectrometry. *J Am Soc Mass Spectrom*. 2015; 26(5):808-817.

35. Bourquard T, Landomiel F, Reiter E, et al. Unraveling the molecular architecture of a G protein-coupled receptor/β-arrestin/Erk module complex. *Sci Rep*. 2015;5(1):10760.

36. Vishnivetskiy SA, Gimenez LE, Francis DJ, et al. Few residues within an extensive binding interface drive receptor interaction and determine the specificity of arrestin proteins. *J Biol Chem*. 2011;286(27):24288-24299.

37. Gimenez LE, Kook S, Vishnivetskiy SA, Ahmed MR, Gurevich EV, Gurevich VV. Role of receptor-attached phosphates in binding of visual and non-visual arrestins to G protein-coupled receptors. *J Biol Chem*. 2012; 287(12):9028-9040.

38. Gimenez LE, Vishnivetskiy SA, Baameur F, Gurevich VV. Manipulation of very few receptor discriminator residues greatly enhances receptor specificity of non-visual arrestins. *J Biol Chem*. 2012;287(35): 29495-29505.

39. Vishnivetskiy SA, Hosey MM, Benovic JL, Gurevich VV. Mapping the arrestin-receptor interface. Structural elements responsible for receptor specificity of arrestin proteins. *J Biol Chem*. 2004;279(2):1262-1268.

40. Raman D, Osawa S, Gurevich VV, Weiss ER. The interaction with the cytoplasmic loops of rhodopsin plays a crucial role in arrestin activation and binding. *J Neurochem*. 2003;84(5): 1040-1050.

41. Shan J, Weinstein H, Mehler EL. Probing the structural determinants for the function of intracellular loop 2 in structurally cognate G-protein-coupled receptors. *Biochemistry*. 2010;49(50):10691-10701.

42. Yang H-S, Sun N, Zhao X, et al. Role of helix 8 in dopamine receptor signaling. *Biomol Ther (Seoul)*. 2019;27(6):514-521.

43. Okada T, Sugihara M, Bondar AN, Elstner M, Entel P, Buss V. The retinal conformation and its environment in rhodopsin in light of a new 2.2 A crystal structure. *J Mol Biol*. 2004;342(2): 571-583.

44. Krieger F, Möglich A, Kiefhaber T. Effect of proline and glycine residues on dynamics and barriers of loop formation in polypeptide chains. *J Am Chem Soc*. 2005;127(10): 3346-3352.

45. Lindström S, Wang L, Smith EN, et al; CHARGE Hemostasis Working Group. Genomic and transcriptomic association studies identify 16 novel susceptibility loci for venous thromboembolism. *Blood*. 2019; 134(19):1645-1657.

46. Kahn ML, Hammes SR, Botka C, Coughlin SR. Gene and locus structure and chromosomal localization of the protease-activated receptor gene family. *J Biol Chem*. 1998;273(36): 23290-23296.

47. Gieseler F, Ungefroren H, Settmacher U, Hollenberg MD, Kaufmann R. Proteinase-activated receptors (PARs) - focus on receptor-receptor-interactions and their physiological and pathophysiological impact. *Cell Commun Signal*. 2013;11(1):86.

48. Han X, Nieman MT. PAR4 (protease-activated receptor 4): Particularly important 4 anti-platelet therapy. *Arterioscler Thromb Vasc Biol*. 2018;38(2):287-289.

49. Zhao P, Metcalf M, Bunnett NW. Biased signaling of protease-activated receptors. *Front Endocrinol (Lausanne)*. 2014;5:67.

50. Khan A, Li D, Ibrahim S, Smyth E, Woulfe DS. The physical association of the P2Y12 receptor with PAR4 regulates arrestin-mediated Akt activation. *Mol Pharmacol*. 2014;86(1):1-11.

51. Lin H, Liu AP, Smith TH, Trejo J. Cofactoring and dimerization of proteinase-activated receptors. *Pharmacol Rev*. 2013;65(4): 1198-1213.

52. Sharma R, Waller AP, Agrawal S, et al. Thrombin-induced podocyte injury is protease-activated receptor dependent. *J Am Soc Nephrol*. 2017;28(9):2618-2630.

53. Smith TH, Li JG, Dores MR, Trejo J. Protease-activated receptor-4 and purinergic receptor P2Y12 dimerize, co-internalize, and activate Akt signaling via endosomal recruitment of β-arrestin. *J Biol Chem*. 2017;292(33): 13867-13878.

54. Whitley MJ, Henke DM, Ghazi A, et al. The protease-activated receptor 4 Ala120Thr variant alters platelet responsiveness to low-dose thrombin and protease-activated receptor 4 desensitization, and is blocked by non-competitive $P2Y_{12}$ inhibition. *J Thromb Haemost*. 2018;16(12):2501-2514.

55. Kimmelstiel C, Stevenson R, Nguyen N, et al. Enhanced potency of prasugrel on protease-activated receptors following bivalirudin treatment for PCI as compared to clopidogrel. *Thromb Res*. 2019;177:59-69.

56. Fotiadis D, Jastrzebska B, Philippsen A, Müller DJ, Palczewski K, Engel A. Structure of the rhodopsin dimer: a working model for G-protein-coupled receptors. *Curr Opin Struct Biol*. 2006;16(2):252-259.

57. Guo W, Shi L, Filizola M, Weinstein H, Javitch JA. Crosstalk in G protein-coupled receptors: changes at the transmembrane homodimer interface determine activation. *Proc Natl Acad Sci U S A*. 2005;102(48):17495-17500.

58. Wang HX, Konopka JB. Identification of amino acids at two dimer interface regions of the alpha-factor receptor (Ste2). *Biochemistry*. 2009;48(30):7132-7139.

59. McMillin SM, Heusel M, Liu T, Costanzi S, Wess J. Structural basis of M3 muscarinic receptor dimer/oligomer formation. *J Biol Chem*. 2011;286(32):28584-28598.

60. Gerszten RE, Chen J, Ishii M, et al. Specificity of the thrombin receptor for agonist peptide is defined by its extracellular surface. *Nature*. 1994;368(6472):648-651.

61. Al-Ani B, Wijesuriya SJ, Hollenberg MD. Proteinase-activated receptor 2: differential activation of the receptor by tethered ligand and soluble peptide analogs. *J Pharmacol Exp Ther*. 2002;302(3):1046-1054.

62. Covic L, Gresser AL, Kuliopulos A. Biphasic kinetics of activation and signaling for PAR1 and PAR4 thrombin receptors in platelets. *Biochemistry*. 2000;39(18):5458-5467.

63. Shapiro MJ, Weiss EJ, Faruqi TR, Coughlin SR. Protease-activated receptors 1 and 4 are shut off with distinct kinetics after activation by thrombin. *J Biol Chem*. 2000;275(33): 25216-25221.

64. Thibeault PE, LeSarge JC, Arends D, et al. Molecular basis for activation and biased signaling at the thrombin-activated GPCR proteinase activated receptor-4 (PAR4). *J Biol Chem*. 2020;295(8):2520-2540.

65. Lodowski DT, Palczewski K, Miyagi M. Conformational changes in the g protein-coupled receptor rhodopsin revealed by histidine hydrogen-deuterium exchange. *Biochemistry*. 2010;49(44):9425-9427.

66. Miyagi M, Wan Q, Ahmad MF, et al. Histidine hydrogen-deuterium exchange mass spectrometry for probing the microenvironment of histidine residues in dihydrofolate reductase. *PLoS One*. 2011;6(2):e17055.

67. Mullangi V, Zhou X, Ball DW, Anderson DJ, Miyagi M. Quantitative measurement of the solvent accessibility of histidine imidazole groups in proteins. *Biochemistry*. 2012;51(36): 7202-7208.

68. Jacques SL, LeMasurier M, Sheridan PJ, Seeley SK, Kuliopulos A. Substrate-assisted catalysis of the PAR1 thrombin receptor. Enhancement of macromolecular association and cleavage. *J Biol Chem*. 2000;275(52): 40671-40678.

69. Bah A, Chen Z, Bush-Pelc LA, Mathews FS, Di Cera E. Crystal structures of murine thrombin in complex with the extracellular fragments of murine protease-activated receptors PAR3 and PAR4. *Proc Natl Acad Sci U S A*. 2007; 104(28):11603-11608.

70. Sánchez Centellas D, Gudlur S, Vicente-Carrillo A, Ramström S, Lindahl TL. A cluster of aspartic residues in the extracellular loop II of PAR 4 is important for thrombin interaction and activation of platelets. *Thromb Res*. 2017; 154:84-92.

71. Boknäs N, Faxälv L, Sanchez Centellas D, et al. Thrombin-induced platelet activation via PAR4: pivotal role for exosite II. *Thromb Haemost*. 2014;112(3):558-565.

72. Lin YC, Ko YC, Hung SC, et al. Selective inhibition of PAR4 (protease-activated receptor 4)-mediated platelet activation by a synthetic nonanticoagulant heparin analog. *Arterioscler Thromb Vasc Biol*. 2019;39(4):694-703.

73. Yu H, Zhao Y, Guo C, Gan Y, Huang H. The role of proline substitutions within flexible regions on thermostability of luciferase. *Biochim Biophys Acta*. 2015;1854(1):65-72.

74. McLaughlin JN, Shen L, Holinstat M, Brooks JD, Dibenedetto E, Hamm HE. Functional selectivity of G protein signaling by agonist peptides and thrombin for the protease-activated receptor-1. *J Biol Chem*. 2005; 280(26):25048-25059.

75. Ramachandran R, Mihara K, Thibeault P, et al. Targeting a proteinase-activated receptor 4 (PAR4) carboxyl terminal motif to regulate platelet function. *Mol Pharmacol*. 2017;91(4): 287-295.

76. O'Brien PJ, Prevost N, Molino M, et al. Thrombin responses in human endothelial cells. Contributions from receptors other than PAR1 include the transactivation of PAR2 by thrombin-cleaved PAR1. *J Biol Chem*. 2000; 275(18):13502-13509.

77. Heenkenda MK, Lindahl TL, Osman A. Frequency of PAR4 Ala120Thr variant associated with platelet reactivity significantly varies across sub-Saharan African populations. *Blood*. 2018;132(19):2103-2106.

78. Morikawa Y, Kato H, Kashiwagi H, et al. Protease-activated receptor-4 (PAR4) variant influences on platelet reactivity induced by PAR4-activating peptide through altered Ca^{2+} mobilization and ERK phosphorylation in healthy Japanese subjects. *Thromb Res*. 2018; 162:44-52.

79. Beckman MG, Hooper WC, Critchley SE, Ortel TL. Venous thromboembolism: a public health concern. *Am J Prev Med*. 2010;38(suppl 4): S495-S501.

80. French SL, Arthur JF, Lee H, et al. Inhibition of protease-activated receptor 4 impairs platelet procoagulant activity during thrombus formation in human blood. *J Thromb Haemost*. 2016;14(8):1642-1654.

81. Vretenbrant K, Ramström S, Bjerke M, Lindahl TL. Platelet activation via PAR4 is involved in the initiation of thrombin generation and in clot elasticity development. *Thromb Haemost*. 2007;97(3):417-424.

82. Duvernay M, Young S, Gailani D, Schoenecker J, Hamm HE. Protease-activated receptor (PAR) 1 and PAR4 differentially regulate factor V expression from human platelets. *Mol Pharmacol*. 2013;83(4):781-792.

83. Hamilton JR, Trejo J. Challenges and opportunities in protease-activated receptor drug development. *Annu Rev Pharmacol Toxicol*. 2017;57(1):349-373.

84. Li S, Tarlac V, Hamilton JR. Using PAR4 inhibition as an anti-thrombotic approach: Why, how, and when? *Int J Mol Sci*. 2019;20(22): 5629.

85. Wilson SJ, Ismat FA, Wang Z, et al. PAR4 (protease-activated receptor 4) antagonism with BMS-986120 inhibits human ex vivo thrombus formation. *Arterioscler Thromb Vasc Biol*. 2018;38(2):448-456.

86. García-Nafría J, Lee Y, Bai X, Carpenter B, Tate CG. Cryo-EM structure of the adenosine A2A receptor coupled to an engineered heterotrimeric G protein. *eLife*. 2018;7: e35946.

87. Zhao DY, Pöge M, Morizumi T, et al. Cryo-EM structure of the native rhodopsin dimer in nanodiscs. *J Biol Chem*. 2019;294(39): 14215-14230.